Progress in PHOTOVOLTAICS

PROGRESS IN PHOTOVOLTAICS: RESEARCH AND APPLICATIONS
Prog. Photovolt: Res. Appl. 2014; **23:**1390–1397
Published online 26 August 2014 in Wiley Online Library (wileyonlinelibrary.com). DOI: 10.1002/pip.2539

APPLICATIONS

Spatial power fluctuation correlations in urban rooftop photovoltaic systems

Boudewijn Elsinga* and Wilfried van Sark

Copernicus Institute, Utrecht University, PO Box 80.115, 3508TC Utrecht, The Netherlands

ABSTRACT

In this paper, we investigate the spatial dependence of variations in power output of small residential solar photovoltaic (PV) systems in a densely populated urban area ($\approx$ 100 km^2) in and around Utrecht, the Netherlands. Research into the geo-statistical behavior of this kind of randomly spaced collection of PV systems is complementary to other studies in the field of compact regularly spaced MW-scale PV plants. Fluctuations in power output between PV systems are correlated up to a certain decorrelation length. Decorrelation is reached (within $1 - e^{-3} \approx 95\%$) in an exponential model and the spatial scale ranges from 100 m to approx. 15 km, with a mean value 0.34($\pm$ 0.2), 2.6($\pm$ 0.3), and 5.0($\pm$ 0.5) km for measurement time step of the time series of respectively 1, 5, and 15 min. These length scales are typical for an urban environment and is important for reduction of variability in aggregated output variability of PV systems. Furthermore, the distance-independent variability *still* itself was found to be strictly linearly dependent on daily mean variability values. This is a good validation of the decorrelation of inter-system ramp rate correlation over distances longer than the characteristic decorrelation length. Copyright © 2014 John Wiley & Sons, Ltd.

KEYWORDS
solar photovoltaics; PV output variability; power fluctuations; spatial correlations

***Correspondence**
Boudewijn Elsinga, Copernicus Institute, Utrecht University, PO Box 80.115, 3508TC Utrecht, The Netherlands.
E-mail: b.elsinga@uu.nl

Received 21 January 2014; Revised 6 June 2014; Accepted 24 June 2014

1. INTRODUCTION

Increasing penetration of intermittent renewable energy sources such as wind and solar photovoltaic (PV) will lead to increased variability on the electricity distribution network [1–6]. This will affect the dispatch patterns of flexible load power generation units, usually reducing their overall energy efficiency. When no changes are made to the existing electricity transmission and distribution network, a ceiling may exist for the further implementation of renewables. A key cause for the short-term (1 s–15 min) intermittency of PV is the passing of clouds. The spatial effect of the movement (and evolution) of clouds translates into correlation of variations of power output by geographically dispersed PV systems [7]. This type of correlation is mentioned by several authors, but usually for large MW-scale PV power plants [8]. The growth in installed PV capacity in the Netherlands is mainly from distributed, privately owned residential rooftop systems because of limited financial incentive and available space [9]. Controlling the variability of this intermittent and distributed supply of electrical power will be necessary for future local (Low and Medium Voltage level) grid stability.

This paper discusses the results of a 1 year study on the variability and correlation of 25 PV systems over an urban area. It further presents results from an exponential model, comparable with the semi-variogram to assess decorrelation distances between PV systems. The use of spatial semi-variograms in the field of irradiation interpolation and forecasting is used by several authors, including [10–12]. The goal of our paper is to quantify the spatial dependence of variability of the power output variations of PV systems. Several studies have been performed on this subject, see, for example, [1,8,13–15] for decorrelation of global irradiation versus inter-station distances in the order of 1–10 km for time intervals of 1–15 min. Depending on the time step size (Δt) used, different characteristic length scales can be recognized due to inclusion of change in power output by passing clouds of different speeds and size. In this paper, we will focus on the measured change in power output versus fixed physical distance to be as close to the realistic AC-power variability as possible. In this study, we disregard wind related effects.

2. METHOD

The data for our research was collected through pulse giving kWh-meters at the AC-side of 25 existing urban rooftop PV systems in the city region of Utrecht (NL), which span an area of approx. 100 km^2 (Figure 1).

The measurements were stored in local data loggers (Leiderdorp Instruments) and transmitted via the general packet radio service network to a central server. From the measured kWh data, Power output and power fluctuation data were derived. Time series measurement resolution was 1 min (cumulative kWh), and averaging over bins of $\Delta t \in \{1, 5, 15\}$ min was applied to improve resolution in the energy domain (from 60W to 12W and 4W), such that:

$$P^{(\Delta t)}(t) = \text{mean}[P(t), P(t+1), \ldots, P(t+\Delta t-1)] \quad (1)$$

Because the same time series starting point is chosen for all the PV systems, aliasing of the Power Output should not be a problem when comparing the different systems, as discussed in Marcos *et al.* 2011 [16].

The power fluctuation is defined as follows:

$$\overline{\Delta \mathrm{P}}_i^{(\Delta t)}(t) = \overline{\mathrm{P}}_i^{(\Delta t)}(t+\Delta t) - \overline{\mathrm{P}}_i^{(\Delta t)}(t) \quad (2)$$

Because the mean is taken in Equation (1), Δt does not appear in the denominator in Equation (2) so the power fluctuation should be regarded as the difference of mean power between subsequent bins of length Δt. The bar indicates normalization to site-specific rated power of PV system i: $\overline{P_i}(t) \equiv P_i(t)/P_{\text{rated},i}$

According to Yordanov *et al.* (2013) [17], a time resolution of around 0.10 s is necessary to incorporate all cloud passing irradiance changes in the south of Norway (where similar climatic conditions prevail as in the Netherlands), so a temporal resolution of either 1 or 5 min can be regarded as having a smoothing effect on the real irradiance variability and thus the PV power output data. However, for this preliminary study, it provides sufficient temporal resolution to investigate PV power output variability. Also the 15 min interval is investigated, as this is the shortest time interval that is of importance on the electricity markets.

Measurements between 8:00 and 19:00 were used, to avoid topographical shading from high solar zenith angles. Power output data of days with measurement gaps or transient power output events that resulted in higher than 140% of the site-specific installed power were discarded. These kind of bad quality data were exclusively related to time stamp mismatching after the general packet radio service signal was interrupted due to sometimes poor signal coverage.

Normalization of the power output data was done relative to the rated power of the PV system, including a mean correction for exponential output degradation of 20% over 25 years. In some cases, the PV panels' installed power was higher than the maximum output of the inverter used.

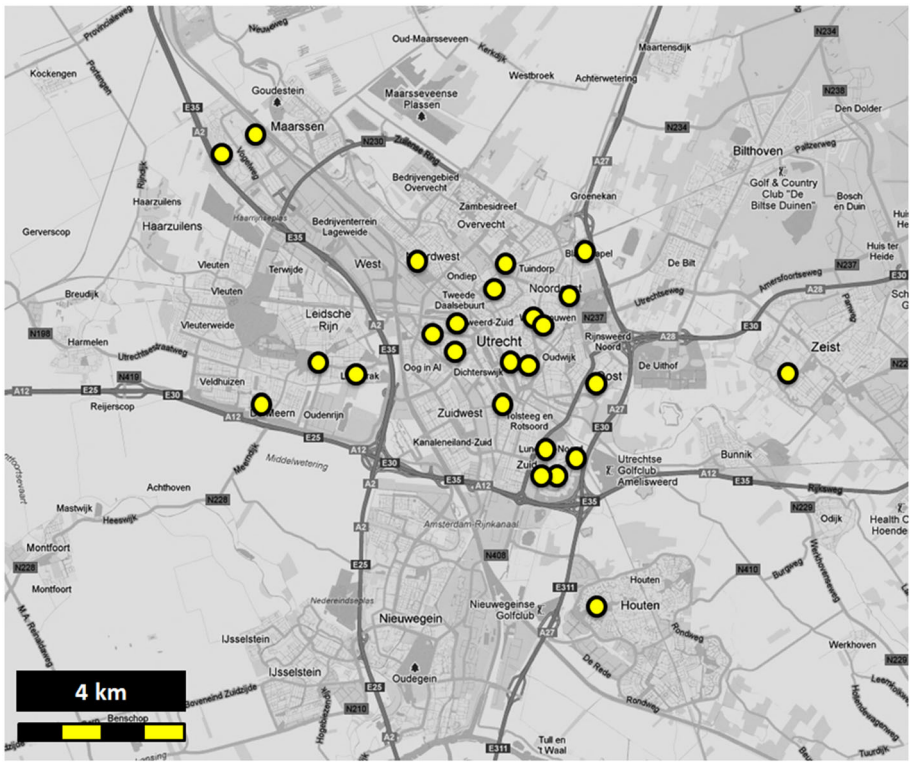

Figure 1. Overview of the photovoltaic systems, located in and around the city of Utrecht (NL). (map data: Google maps 2013).

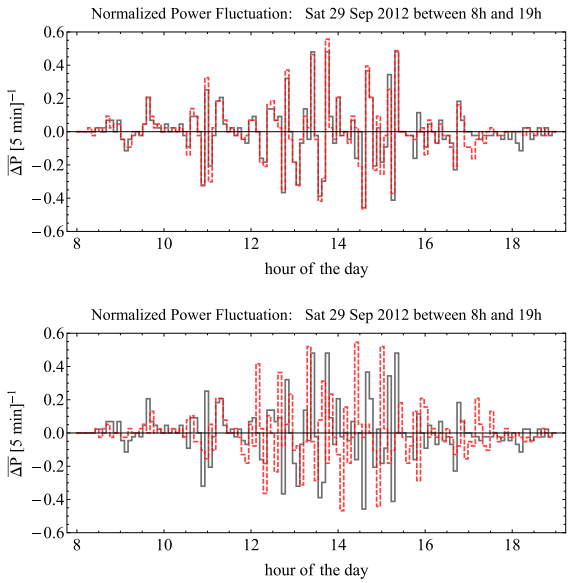

Figure 2. Visualization of $\overline{\Delta P}^{(\Delta t=5\text{min})}$ for two photovoltaic systems on the same day. The top panel shows the $\overline{\Delta P}$ of two locations (full and dashed line) that are located close together ($d_{ij} \approx 160$ m). The bottom panel shows the same location (full line) and another photovoltaic system (dashed line) located 3.6 km away. Clearly, the first pair $\overline{\Delta P}$ behavior is more similar than the second pair, when compared instantaneously; this is an indicator that ΔP's correlation is inversely proportional to inter-system distance.

In those cases, the maximum power output of the inverter was used for normalization.

The measurements comprise a little more than a year from 11 June 2012 through 31 August 2013. This way, all the seasonal variances are captured in the data and a distinction between a summer and winter period can be made. The Dutch climate is very diverse (temperate oceanic), and this means days of high variability are present both in summer and in winter; the same is true for clear sky days. The "summer" period is defined between the last Sunday in March and the last Sunday in October to coincide with the daylight saving offset of +1 hour relative to the Dutch standard time (GMT+1).

2.1. Power fluctuation variance

Correlation of the normalized ΔP data was done between each possible pair i,j of the 25 PV systems, see, for example, Figure 2. Each of these pairs of PV systems represent a geographical distance d_{ij}. For a given pair of PV systems, the normalized power fluctuation time series on a day d within the measurement period at time t and Δt are shown in a scatter plot, in order to define the correlation between them (Figure 3).

Regular (Pearson) covariance, which has been used in previous studies on correlation length scales, for example, Otani *et al.* (1997) [13], Perez *et al.* (2012) [14], and Perpiñan *et al.* (2013) [15], will not be the measure of (de)correlation. In this paper, we propose the following method using the standard deviation parallel and perpendicular to the scattered $\overline{\Delta P}$ data from the pair i,j. This is achieved by applying a rotation matrix of 45° to the data points with respect to the i,j-axes. Of this rotated scatter plot, the variance is calculated; $\mathrm{Var}_{ij,d}^{\overline{\Delta P}\perp}$ and $\mathrm{Var}_{ij,d}^{\overline{\Delta P}\parallel}$ denote the x and y variance of the 45° rotated scatter plot, respectively. The resulting standard deviations are then defined by Equation (3).

$$\sigma_{ij,d}^{(\overline{\Delta P})\perp/\parallel} \equiv \sqrt{\mathrm{Var}_{ij,d}^{\overline{\Delta P}\perp/\parallel}} \tag{3}$$

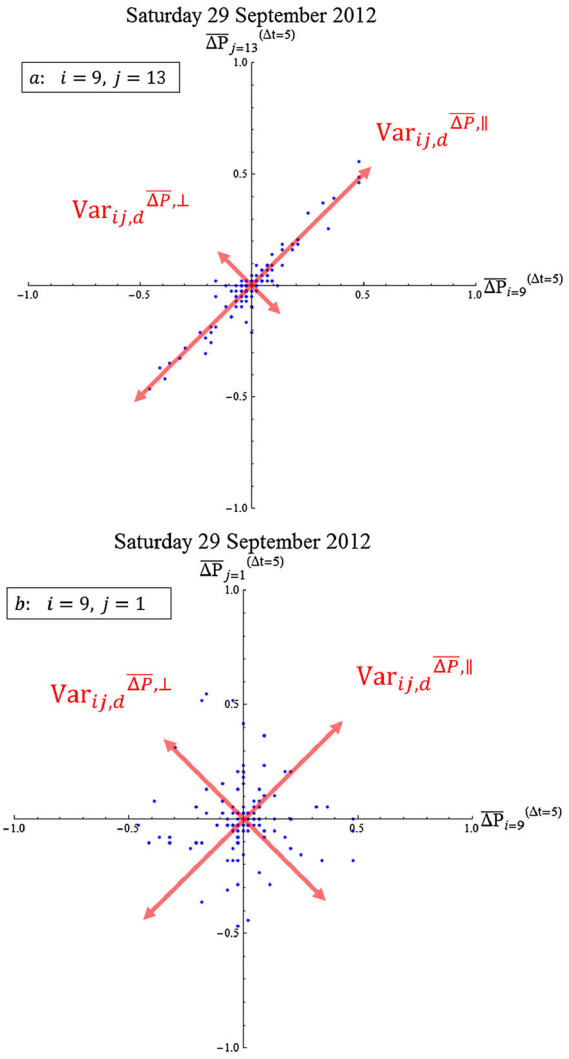

Figure 3. Scatter plot of normalized ΔP values of two PV systems on a variable day (dots). Variances perpendicular and parallel to the $\overline{\Delta P}_{i,d}^{\Delta t} = \overline{\Delta P}_{j,d}^{\Delta t}$ - line are indicated by the arrows. (a) Two closely correlated photovoltaic systems, separated approx. 160 m and (b) two weakly correlated photovoltaic systems, separated approx. 3.6 km.

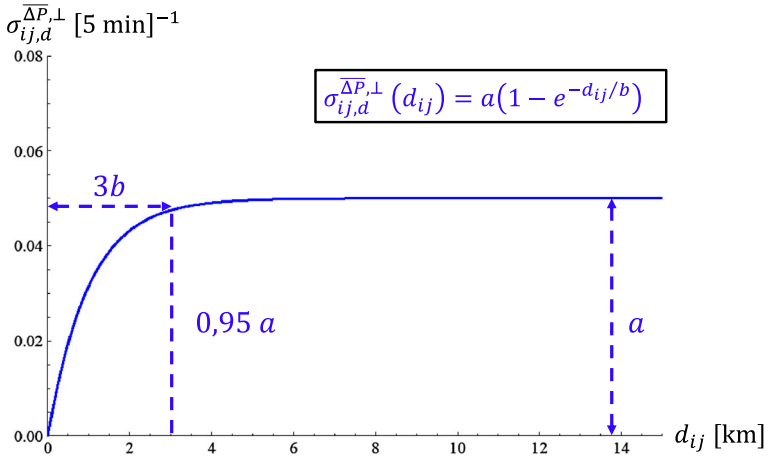

Figure 4. Relevant parameters in the exponential model. Especially 3*b*, the length scale (range) over which the distance-independent constant *still a* is reached within 95%, will be of interest in this study.

Two PV systems that have highly correlated variability will have ΔP-events that coincide within one Δt of the time series and will therefore align on the $\overline{\Delta P}_{i,d}^{(\Delta t)} = \overline{\Delta P}_{j,d}^{(\Delta t)}$-line in such a scatter plot (Figure 3(a)). Deviations from this alignment indicate ΔP-events on different moments from, for example, a cloud that influences the power output and the ΔP of the PV systems successively at different times, increasing the inter-system variance hence reducing the correlation of their power fluctuations (Figure 3(b)).

Looking at $\sigma^{(\overline{\Delta P})\perp}$ and $\sigma^{(\overline{\Delta P})\parallel}$ thus allows for distinguishing the inter-system variability and the overall variability, respectively. The width of the time step Δt not only influences the resolution in the values of the ΔP's, but also the spatial separation over which moving clouds influence different PV systems. A short interval (e.g., 1 min) will only count fast clouds or short distances, whereas a larger interval incorporates the effects of the moving cloud on PV systems that are further apart.

Furthermore, the standard deviation *along* the $\overline{\Delta P}_{i,d}^{(\Delta t)} = \overline{\Delta P}_{j,d}^{(\Delta t)}$-line, for example, the overall output variability, is an indication of spread of the magnitudes of ΔP's on that day d. The mean of the overall output variability of all the i,j pairs on a specific day d, is taken to be the "mean output variability (MOV_d)":

$$\mathrm{MOV}_d \equiv \frac{2}{N(d)^2 - N(d)} \Sigma_{i=1}^{N(d)} \Sigma_{j=i+1}^{N(d)} \sigma_{ij,d}^{(\overline{\Delta P})\parallel}, \qquad (4)$$

with N(d) the available number of systems on that day, and the fraction preceding the summation the result of counting all the different i,j-pairs once, excluding the instances where $i = j$.

2.2. Exponential model

On each day d, the number of available PV systems, $N(d)$, produce $(N(d)^2 - N(d))/2$ values of d_{ij}, and the accompanying $\sigma_{ij,d}^{(\overline{\Delta P})\perp}(d_{ij})$. Each day thus yields a graph, illustrating the relation between the standard deviation of inter-system ΔP variance, $\sigma_{ij,d}^{(\overline{\Delta P})\perp}$ and d_{ij}, which is fitted by an exponential model (Equation (5)).

$$\sigma_{ij,d}^{(\overline{\Delta P})\perp}(d_{ij}) = a\left(1 - e^{-d_{ij}/b}\right) \qquad (5)$$

An example of the generic exponential model is shown in Figure 4. This is comparable with the (exponential) non-stationary semi-variogram, in the context of geo-statistics. The semi-variogram is an essential part of spatial (or spatio-temporal) forecasting (*kriging* [18]) of PV power production, which is the long-term goal of our research.

The exponential model that was used in our study differs from the definition of the semi-variogram because we look at the standard deviation, σ and not the variance σ^2 as the indicator for variability. This way, we can compare our results to other (de)correlation studies as, for example, Perez *et al.* [14] and Perpiñan *et al.* [15]. Furthermore, our research focuses on the use of the variance perpendicular to the scatter plot of the ΔP data for the characterization of variability, as described in Section 2.1.

This exponential model was chosen, because it features autocorrelation of a PV system with itself (decrease monotonously toward $d_{i=j} = 0$) and behaves distance-independent on long distances toward the constant level (*still*) (Equation (6)).

$$\lim_{d_{ij}\downarrow 0} \sigma_{ij,d}^{(\overline{\Delta P})\perp} = 0 \qquad \lim_{d_{ij}\to\infty} \sigma_{ij,d}^{(\overline{\Delta P})\perp} \to constant \qquad (6)$$

It is assumed that the error on the measurements and the microscale variation is zero and hence no "nugget-effect"[†]

[†] The nugget-effect is usually visible through an offset in a semi-variogram due to non-ideal autocorrelation.

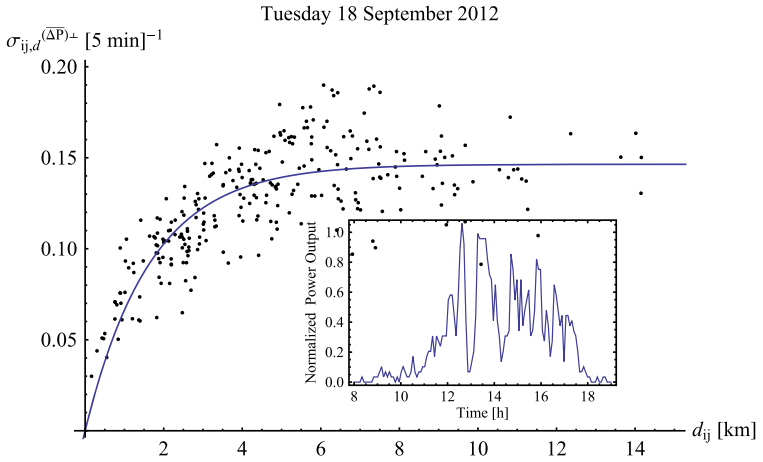

Figure 5. Exponential fit of $\sigma_{ij,d}^{(\overline{\Delta P})\perp}(d_{ij})$ versus inter-system distance d_{ij} on 18-09-2012, a typical variable day. The inset shows an example of a normalized power output time series on that day.

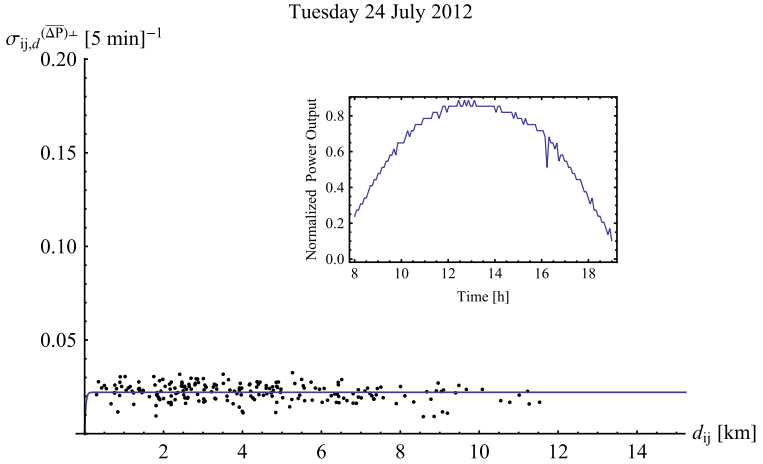

Figure 6. Exponential fit of $\sigma_{ij,d}^{(\overline{\Delta P})\perp}(d_{ij})$ versus inter-system distance d_{ij} on 24-07-2012, a typical clear day. The inset shows an example of a normalized power output time series on that day. Note that the fit, in this case, produces an upper limit to the decorrelation length because the model imposes the existence of the exponential decay, however small it may be.

is present [18]. The second requirement follows from the assumption that clouds (and holes in clouds) are finite in size and will change in size and configuration over the course of transit over an urban region. Therefore, simple (persistent) translation of ΔP-events in the direction of the cloud movement will be insufficient for the description of power output, as indicated as well by Tarroja *et al.* [4]. It is especially this balance between persistence and randomness that defines the characteristic decorrelation length scale within the scope of this paper.

The fit parameters $\{a, b\}$ of the fit model can be graphed versus a qualifier of the variability of the day, such as the MOV_d, giving insight in how correlation parameters depend on the overall irradiance variability on that day.

3. RESULTS AND DISCUSSION

On days with high output variability, a distinct trend is visible in the variability of normalized ΔP's with a significant increase in $\sigma_{ij,d}^{(\overline{\Delta P})\perp}$ and thus a drop in correlation of $(1 - e^{-d_{ij}/b} \approx 95\%)$ over a decorrelation length scale $d_{ij} = 3b$ in the order of a few kilometers (Figure 5). On days with low variability (e.g., 24$^{\text{th}}$ of July 2012 in Utrecht), the decorrelation length shows very different behavior. Because all PV systems behave similar on a clear or completely overcast day, the overall variance is low (a low *still* in the exponential model), and this *still* is independent of the inter-system distance (as can be seen from Figure 6).

DOI: 10.1002/pip

Table I. Decorrelation lengths for different periods and Δt.

	De-correlation length [km] ± (st.dev.)		
Δt	Summer	Winter	Full Year
1 min	0.38 (+/− 0.17)	0.3 (+/− 0.3)	**0.34** (+/− 0.2)
5 min	3.0 (+/− 0.3)	1.9 (+/− 0.3)	**2.6** (+/− 0.3)
15 min	5.4 (+/− 0.6)	4.1(+/− 0.5)	**5.0** (+/− 0.5)

The only variance that is present on days with low variability is due to the finite resolution of the kWh meters measuring PV systems, resulting in stochastic ΔP-events. Hence, ΔP decorrelation is achieved for every inter-system distance and the decorrelation length drops to zero. Sufficiently high resolution and clear sky normalized power output would be very strongly correlated on this kind of day. This will be investigated in future work.

The values found for the decorrelation length, 3*b*, show a large spread which may be due to the fact that cloud movement direction was not included in this study. Furthermore, the PV output data $\overline{P}(t)$ was not normalized to clear sky conditions, and therefore the magnitude of the $\overline{\Delta P}$ was not corrected for orientation and slope.

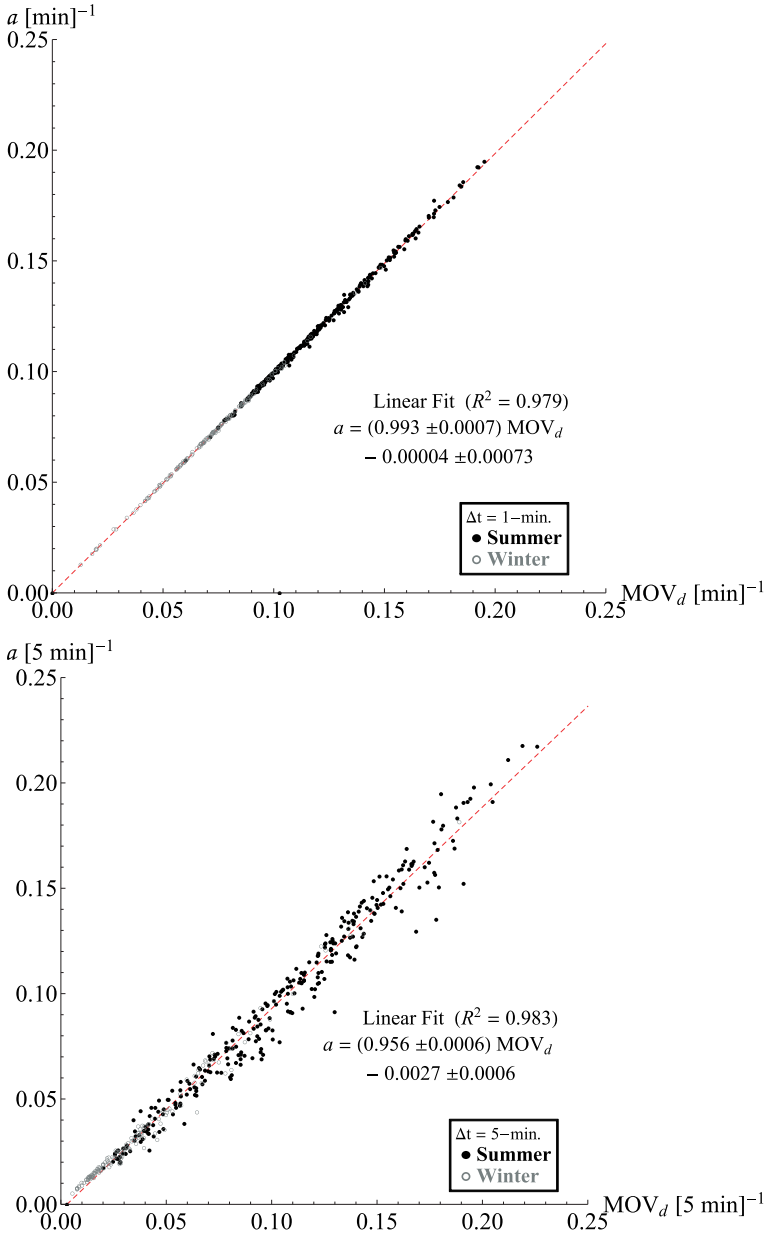

Figure 7. Constant variability *still a* versus daily mean output variability MOV_d, (top: Δt = 1 min, and bottom: Δt = 5 min). The dashed line shows the linear fit for the full year data. The linearity of this fit is a good validation of the used method in this paper.

Values for the decorrelation length range from 100 m to approximately 15 km. The mean value lies between $0.34(\pm 0.2)$ and $5.0(\pm 0.5)$ km for the full year, depending on the time step of the power output time series. These values are an indication that decorrelation is of importance within urban length scales (of $\approx$ 10 km). During the winter period, decorrelation lengths are generally lower than in the summer period or the full year. This can be attributed to the lower variability in PV output as there are more totally overcast days during that period. The summer period contains the more turbulent days with high variability, next to some rare clear sky summer days with lower decorrelation lengths. An overview of the values for the decorrelation length for specific situations is presented in Table I. The presented absolute error (between brackets) is the mean of one standard deviation on the fit model parameters.

The mean $3b$ value is different for the chosen Δt's: structurally higher in the case of (Δt = 5 min and 15 min), indicating that distances over which PV systems are supposed to show correlated $\overline{\Delta P}$-behavior are dependent on the time step that is used in the time series. In other words, variability on a shorter time scale is decorrelated within a more localized area.

The relative error of the found decorrelation lengths, $3b$ in the (Δt = 1 min)-results is significantly higher than in the (Δt = 5 min) or (Δt = 15 min); this is a reflection of the poor raw data resolution of $P^{(1\text{ min.})}(t)$. More detailed (< 1 min) time series data will presumably reduce this error. Additionally, because the PV systems in this paper have different lifetime and levels of maintenance, it was difficult to assess the rated power to normalize them to.

Our results corroborate different studies that use different correlation metrics but arrive nonetheless at similar results. Dependence of decorrelation on Δt is investigated by Perez *et al.* [14] who show decorrelation over $\approx$ 3km within Δt = 5 min, albeit with simulated data. In that study, the effect of cloud movement was incorporated in the dimensionless *dispersion factor*, which will be included in our future work. (Pearson) correlation of wavelets, as discussed in Perpiñan *et al.* (2013) [15], show equally comparable decorrelation length scales using an exponential decay model.

3.1. Distance independent limit

The trend of the *still a*, where dependence on inter-system distance d_{ij} vanishes versus the daily MOV_d is shown in Figure 7. The mean value of the daily MOV_d for the (Δt = 1 min)-results is $0.10(\pm 0.03)$, and for the (Δt = 5 min)-results is $0.08(\pm 0.05)$.

The value a for the distance-independent *still* was found to linearly depend on the MOV_d by a proportionality factor of $0.993(\pm 0.007)$ for (Δt = 1 min), and $0.956(\pm 0.006)$ for (Δt = 5 min). This is an interesting result, given the different nature of both parameters: where MOV_d is the average of the parallel standard deviations of the $\overline{\Delta \text{P}}_{i,j}$-values, and a is found through the *still* of the opposite (perpendicular) standard deviation of the same values. This would indicate that the term "decorrelation length" is correctly chosen: for when the inter-system distance d_{ij} is large enough, the PV systems behave independently, and the $\sigma_{ij,d}^{(\overline{\Delta \text{P}})\perp}$ reflects the same variability information as the $\sigma_{ij,d}^{(\overline{\Delta \text{P}})\parallel}$ does. In other words, the linear fit corroborates Equation (7), where the left hand side reduces to a when looking at Equation (5) where $d_{ij} \gg b$.

$$\lim_{d_{ij} \gg b} \sigma_{ij,d}^{(\overline{\Delta \text{P}})\perp}(d_{ij}) \approx \text{Mean}\left(\sigma_{ij,d}^{(\overline{\Delta \text{P}})\parallel}\right) = \text{MOV}_d \quad (7)$$

4. CONCLUSION

This paper shows that for a collection of randomly spaced urban residential rooftop PV systems in Utrecht (NL) covering an area of $\approx$ 100 km^2, the decorrelation length over which power fluctuation variability becomes distance-independent (defined as $3b$ in the exponential model) ranges from 100 m to approx. 15 km, with a mean value for the full year data of $0.34(\pm 0.2)$, $2.6(\pm 0.3)$, and $5.0(\pm 0.5)$ km, for time step of the time series of respectively 1, 5, and 15 min. The distance-independent variability (*still*, defined as a in the exponential model) was found to linearly depend on the mean output variability by a proportionality factor of $0.993(\pm 0.007)$ for Δt = 1 min and $0.956(\pm 0.006)$ for Δt = 5 min. This shows that the exponential model parameter a is a good proxy for daily variability. This is a validation of the decorrelation of inter-system $\overline{\Delta \text{P}}_{i,j}$-events over distances longer than the characteristic decorrelation length.

This paper shows that the chosen measure for inter-system variability, $\sigma_{ij,d}^{(\overline{\Delta \text{P}})\perp}$ and the found decorrelation length scales are in accordance with similar research on solar PV variability, for example, Perez *et al.* [14]. These results are beneficial to the integration of decentralized (urban rooftop) PV systems into the electricity grid. Decorrelation length scales of PV output variability will be important in the coupling of forecast PV output and demand side management in future smart grid situations.

5. FURTHER RESEARCH

We will extend the current 25 PV systems that are monitored to 200 PV systems, equipped with more sensitive measurement devices; both in the time and in the power domain to reduce measurement error and enable the investigation of the dependence of the found decorrelation lengths on Δt. These data will be accompanied by meteorological measurements and whole-sky cloud imaging techniques for determination of cloud speed and direction, as is done by Lonij *et al.* [19]. Further research will focus on incorporating two-dimensional wind vector data, including a generalization of the dispersion factor that was

DOI: 10.1002/pip

introduced by Hoff and Perez [8] to make ΔP correlation independent of the given weather situation. This will lead to the development of a general model for ΔP correlation in generic randomly distributed PV systems.

ACKNOWLEDGEMENTS

This preliminary study was made possible by funding from the UU *Dean Policy Budget* as well as The Netherlands Enterprise Agency (RVO), who are funding the project *Solar Forecasting & Smart Grids* within the framework of the Dutch Topsector Energy, "TKI Switch2SmartGrids". The authors would like to thank the owners of the PV systems in Utrecht, Maarssenbroek, De Meern, Houten, Zeist and De Bilt (NL) for enabling the measurements.

REFERENCES

1. Mills A, Wiser R. Implications of wide-area geographic diversity for short-term variability of solar power. LBNL-3884E E.O.L. *Report*, Berkeley National Laboratory, 2010.
2. Wiemken E, Beyer HG, Heydenreich W, Kiefer K. Power characteristics of PV ensembles: experiences from the combined production of 100 grid connected PV systems distributed over the area of germany. *Solar Energy* 2001; **70**(6): 513–518.
3. Lave M, Kleissl J, Arias-Castro E. High-frequency irrandiance fluctuations and geographic smoothing. *Solar Energy* 2012; **86**: 2190–2199.
4. Tarroja B, Mueller F, Samuelsen S. Solar power variability and spatial diversification: implications from an electric grid load balancing perspective. *International Journal of Energy Research* 2012; **37**(9): 1002–1016.
5. Marcos J, Marroyo L, Lorenzo E, García M. Smoothing of PV power fluctuations by geographical dispersion. *Progress in Photovoltaics: Research and Applications* 2012; **20**: 226–237. DOI: 10.1002/pip.1127
6. ElNozahy MS, Salama MMA. Technical impacts of grid-connected photovoltaic systems on electrical networks - A review. *Journal of Renewable and Sustainable Energy* 2013; **5** (032702): DOI: 10.1063/1.4808264
7. Lave M, Kleissl J. Solar variability of four sites across the state of Colorado. *Renewable Energy* 2010; **35**: 2867–2873.
8. Hoff TE, Perez R. Quantifying PV power output variability. *Solar Energy* 2010; **84**: 1782–1793.
9. Van Sark WGJHM, Muizebelt P, Cace J, De Vries A, De Rijk P. Price development of photovoltaic modules, inverters and systems in the Netherlands in 2012. *Renewable Energy* 2014; **71**: 18–22.
10. Sen Z, Sahin AD. Spatial interpolation and estimation of solar irradiation by cumulative semivariograms. *Solar Energy* 2001; **7**(1): 11–21.
11. Inoue T, Sasaki T, Washio T. Spatio-temporal kriging of solar radiation incorporating direction and speed of cloud movement, In *26th Annual Conference of the Japanese Society for Artificial Intelligence*, Yamaguchi city, 2012; 1K2-IOS-1b-3.
12. Yang D, Chaojun G, Dong Z, Jirutitijaroen P, Chen N, Walsh WM. Solar irradiance forecasting using spatial-temporal covariance structures and time-foreward kriging. *Renewable Energy* 2013; **60**: 235–245.
13. Otani K, Minowa J, Kosuke K. Study on areal solar irradiance for analyzing areally-totalized PV systems. *Solar Energy Materials and Solar Cells* 1997; **47**: 281–288.
14. Perez R, Schlemmer J, Kivalov S, Hemker K, Jr., Hoff TE. Short-term irradiance variability: preliminary estimation of station pair correlation as a function of distance. *Solar Energy* 2012; **86**: 2170–2176.
15. Perpiñan O, Marcos J, Lorenzo E. Electrical power fluctuations in a network of DC/AC inverters in a large pv plant: relation between correlation, distance and time scale. *Solar Energy* 2013; **88**: 227–241.
16. Marcos J, Marroyo L, Lorenzo E, Alvira D, Izco E. Power output fluctuations in large scale PV plants: one year observations with one second resolution and a derived analytic model. *Progress in Photovoltaics: Research and Applications* 2011; **19**: 218–227. DOI: 10.1002/pip.1016
17. Yordanov GH, Saetre TO, Midtgard O. Optimal temporal resolution for detailed studies of cloud-enhanced sunlight (overirradiances), In *39th IEEE PVSC Proceedings*, Tampa, Florida (US), 2013; 985–988.
18. Cressie N, Wilke CK. In *Statistics for Spatio-Temporal Data*. Wiley & Sons: Hoboken New Jersey, 2011; 124–133.
19. Lonij VPA, Jayadevan VT, Brooks AE, Rodriguez JJ, Koch K, Leuthold M, Cronin AD. Forecasts of PV output using power measurements of 80 residential PV installs, In *38th IEEE PVSC Proceedings*, Austin, Texas (US), 2012; 3300–3305.